Tokamak SOL fluid simulations with self-consistent boundary conditions at the magnetic presheath edge

J. Loizu, F. Halpern, S. Jolliet, A. Mosetto, and P. Ricci

Ecole Polytechnique Fédérale de Lausanne (EPFL), Centre de Recherches en Physique des Plasmas,
Association Euratom-Confédération Suisse, CH-1015 Lausanne, Switzerland

1. Introduction and Motivation

- Global 3D fluid simulations of SOL plasma turbulence are presented using the GBS code [1].
- Interplay between the plasma outflow from the core, perpendicular transport and parallel losses at the limiter.
- No separation between equilibrium and fluctuating quantities.
- **Boundary conditions** at the limiter strongly affect several properties of the plasma, imposing the plasma losses at the wall and therefore the steady state profiles and the plasma circulation.

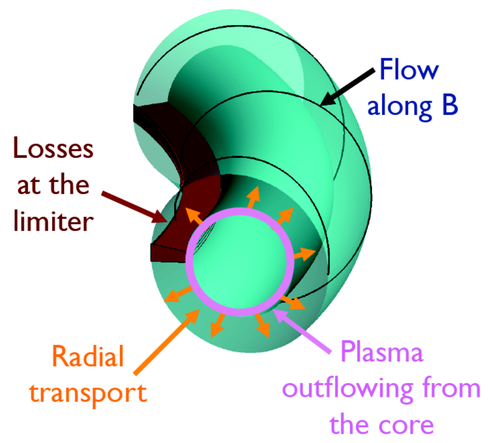

2. Progressive approach using basic plasma physics devices

- GBS has been used for simulating basic plasma physics devices of increasing complexity: linear devices (LAPD, HelCat) [2] and Simple Magnetized Toroidal plasmas (TORPEX, Helimak) [3].

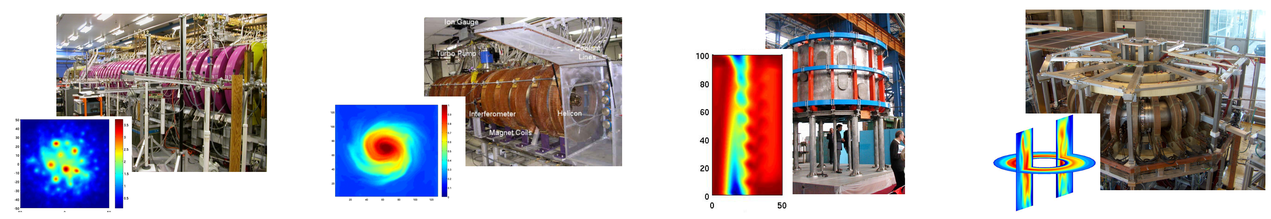

LAPD HelCat Helimak TORPEX

- Unstable linear modes, saturation mechanism, biasing effects have been analyzed.
- We are now approaching the description of the tokamak SOL, by starting from a simple setup.

3. Simulation model

- Drift-reduced Braginskii equations [4] with cold ion approximation $T_i = 0$

$$
\begin{aligned}
\frac{\partial n}{\partial t} &= -\frac{R_0}{B}[\phi, n] + \frac{2}{B}[C(p_e) - C(\phi)] - \nabla\cdot(nV_{\|e}\mathbf{b}_0) + S_n \\
\frac{\partial \omega}{\partial t} &= -\frac{R_0}{B}[\phi, \omega] - V_{\|i}\mathbf{b}_0\cdot\nabla\omega + \frac{B^2}{n}\nabla\cdot(j_\|\mathbf{b}_0) + \frac{2B}{n}C(p_e) + \frac{B}{3n}C(G_i) \\
\frac{\partial \chi}{\partial t} &= -\frac{R_0}{B}[\phi, V_{\|e}] - V_{\|e}\mathbf{b}\cdot\nabla V_{\|e} + \frac{m_i}{m_e}\left(\nu\frac{j_\|}{n} + \mathbf{b}\cdot\nabla\phi - \frac{1}{n}\mathbf{b}\cdot\nabla p_e - 0.71\mathbf{b}\cdot\nabla T_e - \frac{2}{3n}\mathbf{b}\cdot\nabla G_e\right) \\
\frac{\partial V_{\|i}}{\partial t} &= -\frac{R_0}{B}[\phi, V_{\|i}] - V_{\|i}\mathbf{b}\cdot\nabla V_{\|i} - \frac{1}{n}\mathbf{b}\cdot\nabla p_e - \frac{2}{3n}(\vec{b}\cdot\nabla)G_i + \mathcal{D}_{V_{\|i}}(V_{\|i}) \\
\frac{\partial T_e}{\partial t} &= -\frac{R_0}{B}[\phi, T_e] - V_{\|e}\mathbf{b}\cdot\nabla T_e + \frac{4T_e}{3B}\left[\frac{1}{n}C(p_e) + \frac{5}{2}C(T_e) - T_eC(\phi)\right] \\
&\quad + \frac{2T_e}{3}\left[0.71\nabla\cdot(j_\|\mathbf{b}_0) - \nabla\cdot(V_{\|e}\mathbf{b}_0)\right] + \mathcal{D}_{T_e}(T_e) + \mathcal{D}^\|_{T_e}(T_e) + S_{T_e}
\end{aligned}
$$

with

$$
\begin{aligned}
\nabla^2_\perp\phi &= \omega, \quad \vec{\nabla}^2_\perp\delta\psi = \frac{4\pi e}{c}n(V_{\|i} - V_{\|e}), \quad \chi = V_{\|e} + \frac{m_i}{m_e}\frac{\beta}{2}\delta\psi, \\
G_i &= -\eta_{0i}\left[2\mathbf{b}_0\cdot\nabla V_{\|i} + \frac{1}{B}C(\phi)\right] \\
G_e &= -\eta_{0e}\left[2\mathbf{b}_0\cdot\nabla V_{\|e} + \frac{1}{B}\left(\frac{1}{n}C(p_e) + C(\phi)\right)\right] \\
\mathbf{b}\cdot\nabla A &= \mathbf{b}_0\cdot\nabla A + \frac{\beta_e}{2}\frac{R_0}{B}[\delta\psi, A], \\
C(A) &= \frac{B}{2}\left(\nabla\times\frac{\mathbf{b}}{B}\right)\cdot\nabla A, \quad [A, B] = \mathbf{b}\cdot(\nabla A\times\nabla B)
\end{aligned}
$$

- Circular concentric magnetic surfaces:

$$\vec{B}_0 = \frac{B_a R_0}{R}\left(\vec{e}_\varphi + \frac{\epsilon}{q\sqrt{1-\epsilon^2}}\vec{e}_\theta\right)$$

- Local magnetic shear:

$$\partial_x \to \partial_x + (y/a)\hat{s}\partial_y$$

- Toroidal limiter
- Localized n and T_e sources around x_0

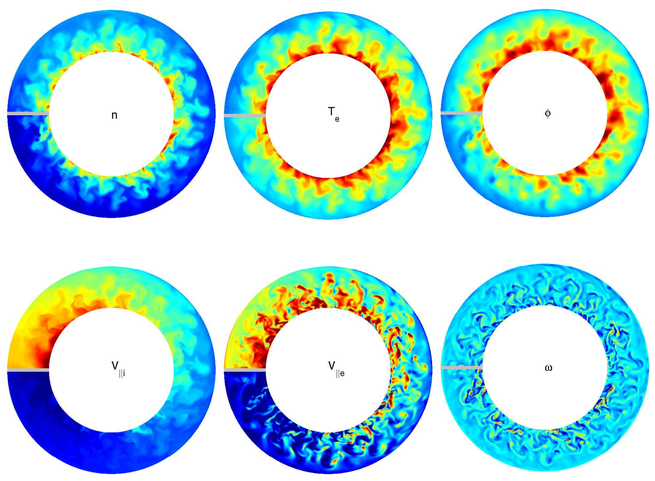

4. Boundary conditions at the magnetic presheath entrance

- Based on a recent theory [5,6], a complete set of boundary conditions at the MPE is derived.

$$
\begin{aligned}
v_{\|i} &= c_s\left[\pm 1 + \theta_n \mp \frac{1}{2}\theta_{T_e} - \frac{2\phi}{T_e}\theta_\phi\right] \\
v_{\|e} &= c_s\left[\pm\exp(\Lambda - \eta_m) - \frac{2\phi}{T_e}\theta_\phi + 2(\theta_n + \theta_{T_e})\right] \\
\partial_s\phi &= -c_s\left[\pm 1 + \theta_n \pm \frac{1}{2}\theta_{T_e}\right]\partial_s v_{\|i} \\
\partial_s n &= -\frac{n}{c_s}\left[\pm 1 + \theta_n \pm \frac{1}{2}\theta_{T_e}\right]\partial_s v_{\|i} \\
\partial_s T_e &= 0 \\
\omega &= -\cos^2\alpha\left[\left[1 + \theta_{T_e}\right](\partial_s v_{\|i})^2\right. \\
&\quad \left. + c_s\left[\pm 1 + \theta_n \pm \theta_{T_e}/2\right]\partial_s^2 v_{\|i}\right]
\end{aligned}
$$

with

$$\theta_A = \frac{c_s}{2\tan\alpha}\frac{\partial_x A}{A}$$

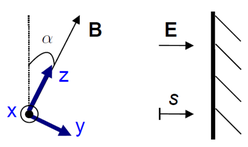

- This set is fully consistent with kinetic simulations of the plasma-wall transition [7].
- These boundary conditions faithfully supply the sheath physics to fluid codes that are based on the ion drift-approximation.

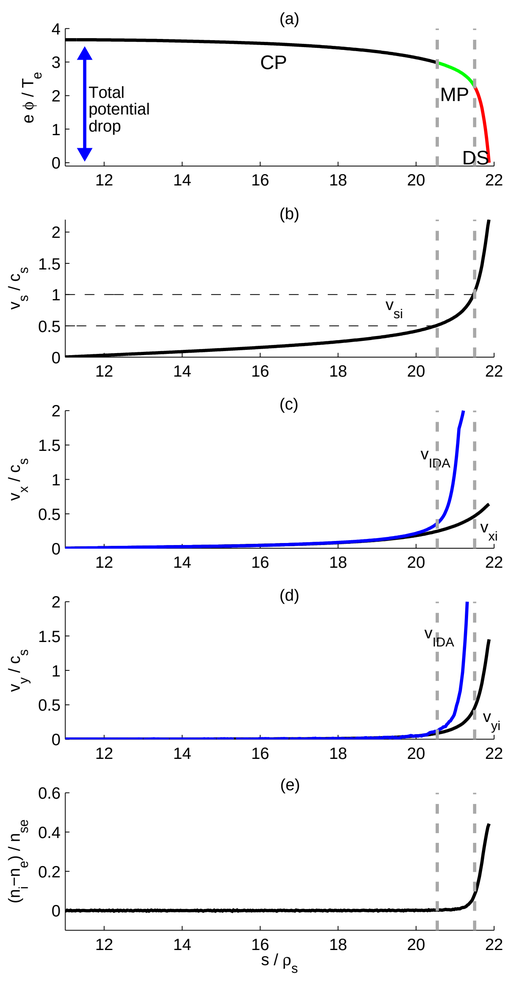

5. SOL equilibrium

- **Motivation:** Combining model equations and b.c., SOL equilibrium profiles can be estimated analytically.
- Time and toroidal average n, T_e and $V_{\|i}$ equations
- Retain dominant terms according to simulations
- $P_A = -\frac{R}{\rho_{s0}}\frac{1}{B}\left[\langle[\tilde{\phi}, \tilde{A}]\rangle_{t,\varphi} + \langle[\bar{\phi}, \bar{A}]\rangle_{t,\varphi}\right]$

$$
\begin{aligned}
P_n - \bar{n}\alpha\frac{\partial}{\partial y}\bar{V}_{\|e} - \bar{V}_{\|e}\alpha\frac{\partial}{\partial y}\bar{n} &= 0 \\
P_{T_e} - \bar{V}_{\|e}\alpha\frac{\partial}{\partial y}\bar{T}_e - \frac{2\bar{T}_e}{3}\alpha\frac{\partial}{\partial y}\bar{V}_{\|e} &= 0 \\
P_{V_{\|i}} - \bar{V}_{\|i}\alpha\frac{\partial}{\partial y}\bar{V}_{\|i} - \left[\alpha\frac{\partial}{\partial y}\bar{T}_e + \frac{\bar{T}_e}{\bar{n}}\alpha\frac{\partial}{\partial y}\bar{n}\right] &= 0
\end{aligned}
$$

- Linearize in x (radial), Taylor expand in y (poloidal)
- Assume $V_{\|i} \approx V_{\|e}$
- Consider turbulent transport only to zeroth order

$$
\begin{aligned}
\bar{n}(y) &= n_0\left(1 + \frac{4}{7}\frac{u_0}{\sqrt{t_0}}\frac{y}{L_y} - \frac{y^2}{L_y^2}\right) \\
\bar{T}_e(y) &= t_0\left(1 + \frac{18}{35}\frac{u_0}{\sqrt{t_0}}\frac{y}{L_y} - \frac{3}{4}\frac{y^2}{L_y^2}\right) \\
\bar{V}_{\|e}(y) &= \sqrt{t_0}\left(\frac{u_0}{\sqrt{t_0}} + 2\frac{y}{L_y} + \frac{16}{7}\frac{y^3}{L_y^3}\right)
\end{aligned}
$$

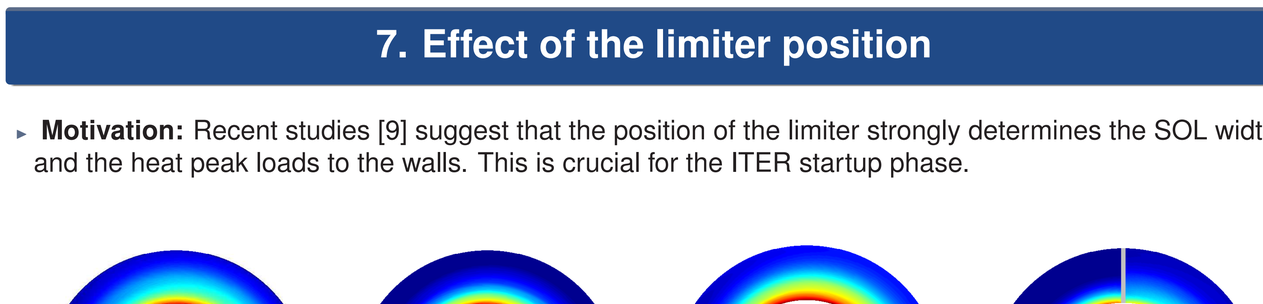

6. Intrinsic rotation

- **Motivation:** Intrinsic rotation in L-mode may be driven by scrape-off-layer flows [8].
- The boundary conditions for $V_{\|i,e}$ drive spontaneous toroidal rotation in the SOL.

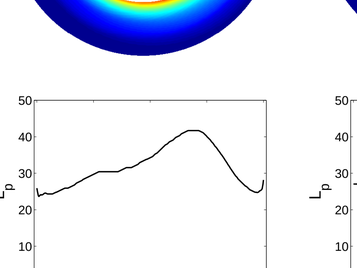

Co-current toroidal rotation

$$M_\varphi \sim \frac{qR}{a}\left(\frac{1}{2}\frac{\rho_s}{L_n} + \frac{1}{4}\frac{\rho_s}{L_T} - \Lambda\frac{\rho_s}{L_\phi}\right)$$

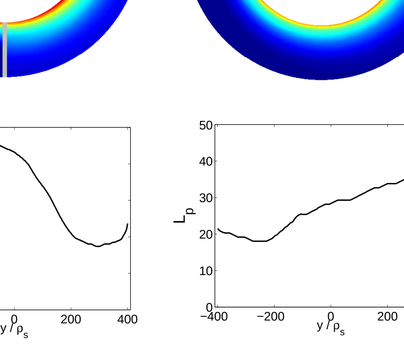

- Simulations performed with $q = 2, 4, 8$ (thus varying α) and with different limiter positions (thus varying $L_\perp$)

7. Effect of the limiter position

- **Motivation:** Recent studies [9] suggest that the position of the limiter strongly determines the SOL width and the heat peak loads to the walls. This is crucial for the ITER startup phase.

8. References

[1] P. Ricci *et al.*, accepted in Plasma Phys. Contr. Fusion
[2] B. N. Rogers and P. Ricci, Phys. Rev. Lett. 104, 225002 (2010)
[3] P. Ricci and B. N. Rogers, Phys. Rev. Lett. 104, 145001 (2010)
[4] A. Zeiler *et al.*, Phys. Plasmas 4, 2134 (1997)
[5] J. Loizu *et al.*, Phys. Rev. E 83, 016406 (2011)
[6] J. Loizu *et al.*, Phys. Plasmas 19, 083507 (2012)
[7] J. Loizu *et al.*, submitted to Phys. Plasmas
[8] B. LaBombard,*et al.*, Nucl. Fusion 52, 045010 (2004)
[9] M. Kocan *et al.*, Plasma Phys. Control. Fusion 52, 045010 (2010)

joaquim.loizu@epfl.ch